Habitability of the early Earth: Liquid water under a faint young Sun facilitated by strong tidal heating due to a nearby Moon

René Heller · Jan-Peter Duda · Max Winkler · Joachim Reitner · Laurent Gizon

Draft July 7, 2020

Abstract Geological evidence suggests liquid water near the Earth's surface as early as 4.4 gigayears ago when the faint young Sun only radiated about 70 % of its modern power output. At this point, the Earth should have been a global snowball. An extreme atmospheric greenhouse effect, an initially more massive Sun, release of heat acquired during the accretion process of protoplanetary material, and radioactivity of the early Earth material have been proposed as alternative reservoirs or traps for heat. For now, the faint-young-sun paradox persists as one of the most important unsolved problems in our understanding of the origin of life on Earth. Here we use astrophysical models to explore the possibility that the new-born Moon, which formed about 69 million years (Myr) after the ignition of the Sun, generated extreme tidal friction – and therefore heat – in the Hadean

---

R. Heller
Max Planck Institute for Solar System Research, Justus-von-Liebig-Weg 3, 37077 Göttingen, Germany
E-mail: heller@mps.mpg.de

J.-P. Duda
Göttingen Centre of Geosciences, Georg-August-University Göttingen, 37077 Göttingen, Germany
E-mail: jan-peter.duda@geo.uni-goettingen.de

M. Winkler
Max Planck Institute for Extraterrestrial Physics, Giessenbachstraße 1, 85748 Garching, Germany
E-mail: winkler@mpe.mpg.de

J. Reitner
Göttingen Centre of Geosciences, Georg-August-University Göttingen, 37077 Göttingen, Germany
Göttingen Academy of Sciences and Humanities, 37073 Göttingen, Germany
E-mail: jreitne@gwdg.de

L. Gizon
Max Planck Institute for Solar System Research, Justus-von-Liebig-Weg 3, 37077 Göttingen, Germany
Institute for Astrophysics, Georg-August-University of Göttingen, Friedrich-Hund-Platz 1, 37077 Göttingen, Germany
E-mail: gizon@mps.mpg.de

and possibly the Archean Earth. We show that the Earth-Moon system has lost $\sim 3 \times 10^{31}$ J, (99 % of its initial mechanical energy budget) as tidal heat. Tidal heating of $\sim 10\,\mathrm{W\,m^{-2}}$ through the surface on a time scale of 100 Myr could have accounted for a temperature increase of up to 5 C° on the early Earth. This heating effect alone does not solve the faint-young-sun paradox but it could have played a key role in combination with other effects. Future studies of the interplay of tidal heating, the evolution of the solar power output, and the atmospheric (greenhouse) effects on the early Earth could help in solving the faint-young-sun paradox.

Keywords early Earth · Tides · Moon · Faint-young-sun paradox · Tidal brittle formation

1 Introduction

Geological records, such as oxygen isotope ($\delta^{18}O$) data from zircons, show that liquid water was present on the Earth's surface as early as 4.4 billion years ago (gigayears ago, Ga)[1] (Mojzsis et al., 2001; Wilde et al., 2001; Valley et al., 2014). This water would not have been pure water near room temperature and pressure but a high-temperature (300 K–450 K) and high-pressure (∼500 bar) mix of H_2O and CO_2. Liu (2004) suggested that CO_2 was then removed continuously over ∼100 Myr to form carbonate rocks. Life could have been present as early as 3.8 Ga to 3.5 Ga as suggested by possible biosignatures preserved in ancient rocks (Schidlowski, 1988; Rosing, 1999), and diverse aquatic life was certainly established by 3.5 Ga - 3.4 Ga as for instance evidenced by organic biosignatures and fossil microbial mats (Lowe, 1980; Walter et al., 1980; Allwood et al., 2006; van Kranendonk, 2011; Duda et al., 2016, 2018; Hickman-Lewis et al., 2018; Homann, 2019). $^{18}O/^{16}O$ isotope ratios in marine cherts and carbonates suggests Archean ocean temperatures between 50° and 85° (Knauth, 2005), although longevity and extent of these conditions remain unclear. Moreover, no evidence for glaciations exist until about 2.9 Ga (von Brunn and Gold, 1993; Young et al., 1998; van Kranendonk et al., 2012).

As example of liquid surface water on the early Earth, Fig. 1 shows the 3.49 Ga North Star Basalt in the Pilbara region (Western Australia), which has pillow structures (Hickman, 1977) and thus evidently formed in aquatic environments. The North Star Basalt and other Paleoarchean pillowed basalts in this area (e.g., Mount Ada Basalt, Apex Basalt, Euro Basalt) are typically crosscut by numerous chert veins, which record hydrothermal pumping of surface water through early Earths crust ("hydrothermal pump hypothesis"; Duda et al., 2018).

As conclusive as the geological record is in regard to the presence of liquid water at (or near) the surface during the first billion years after the formation of the Earth, there is an astrophysical prediction that is in strong disagreement with these observations. Until about 3.5 Ga, the solar illumination on Earth was only

---

[1] Throughout this manuscript we use two time scales, one of which is typically used in astrophysics and one of which is often used in Earth sciences. The first one is the time after formation of the Sun, measured in units of millions of years (Myr) or billions of years (Gyr). The second one is the time before present, with units abbreviated as "Ga" for giga-annum (Arndt, 2011). We use Ga for "gigayears ago" or "gigayears old". For the conversion between the time scales we use a solar age of 4.567 (± 0.06) Gyr determined from $^{204}Pb/^{206}Pb$ vs. $^{207}Pb/^{206}Pb$ isotope measurements in the Allende meteorite (Amelin and Krot, 2007).

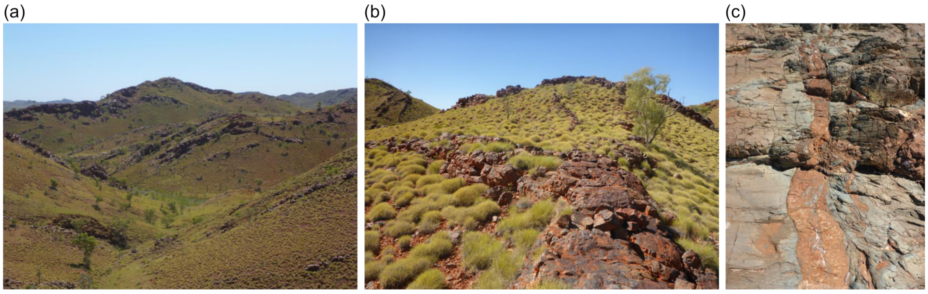

Fig. 1 (a) Early Archean basaltic rocks in the Pilbara region (Western Australia). These rocks evidently formed in aquatic environments as evidenced by pillow structures. Furthermore, pillow basaltic rocks such as the 3.49 Ga North Star Basalt are typically crosscut by numerous chert veins, which record intensive hydrothermal pumping of surface water through the crust at that time ("hydrothermal pump hypothesis"; Duda et al., 2018). (b) Detailed outcrop pattern of black chert veins. The vein in the front has a diameter of about two to three meters. (c) Remarkably, these strata also show other types of evidence for brittle deformation such as widespread carbonate cemented fractures such as this 3.47 Ga Mount Ada Basalt. The brown color of the carbonate is characteristic for Fe-rich dolomites (ankerite). It appears plausible that such features are the product of strong tidal forces exerted by the much closer moon.

about 70 % of its current value. With the solar radiation being the major energy source by far, simple energy balance calculations show that the reduction of the solar luminosity by 30 % compared to its modern value should have led to a global snowball Earth for at least the first billion years or so (Sagan and Mullen, 1972; Kasting et al., 1988).

One possibility to prevent global glaciation is through hugely enhanced atmospheric CO_2 levels. Levels of 100 to 1000 times the present value have been shown theoretically to prevent a global snowball under a faint Sun 2.5 Gyr ago (Kuhn and Kasting, 1983; Kasting, 1987). This would correspond to CO_2 partial pressures of between 0.03 bar and 0.3 bar, compared to 5×10^{-4} bar today. Even more massive amounts of CO_2 with up to between 10 bar and 100 bar of a CO_2-CO dominated atmosphere have been suggested on the Hadean Earth (4.4 Ga - 4 Ga) using model calculations (Nisbet and Sleep, 2001). The lower end of this range overlaps with theoretical estimates of between 1 bar (Miller and Urey, 1959) and 10 bar (Walker, 1983) from atmosphere evolution models and with estimates for the CO_2 inventory could have been stored in the lithosphere (Sagan and Chyba, 1997).

Alternatively, a 1 bar atmosphere with a 10^{-5} volume mixing ratio of NH_3 could have generated the required magnitude of a strong greenhouse effect (Sagan and Mullen, 1972). NH_3, however, would be photodissociated through solar UV radiation on a time scale of just about 40 yr (Kuhn and Atreya, 1979) if it were not continuously supplied in adequate quantities by abiotic processes (Kasting, 1982). Photodissociative destruction of NH_3 could also have been prevented by an UV-opaque high-altitude haze composed of organic solids that were produced from CH_4 photolysis (Sagan and Chyba, 1997). Moreover, CH_4 itself could have acted as an efficient greenhouse gas on the early Earth (Haqq-Misra et al., 2008). This argument, however, shifts the problem to the production of CH_4. Where did it come from? If the only viable source of large amounts of CH_4 is through methanogenic microorganisms (Pavlov et al., 2000; Kasting and Siefert, 2002), then this is a chicken-and-egg dilemma: life would be required to create and maintain the conditions for it to have emerged in the first place.

Other explanations to solve the faint-young-sun paradox include the assumption of a much more massive Sun 4.5 Ga (Whitmire et al., 1995), a much lower fractional land coverage on Earth during the Archean (Flament et al., 2008), and different altitudinal distribution than today, all of which would affect the global albedo (Goldblatt and Zahnle, 2011).

The atmospheric composition of the early Earth and the possibility of a greenhouse effect that is much stronger than the contemporary warming of +33°C compared to an airless body (or of +20.3°C compared to a gray atmosphere model, see Sect. 2.2) could certainly have played important roles in preventing a global snowball Earth. A specific interplay of various chemical, geothermal, and possibly biotic effects (at least once life was present) could solve the problem.

There is, however, a more apparent effect that has, to our perception, been underappreciated (Feulner, 2012) or even overlooked (Charnay et al., 2020; Catling and Zahnle, 2020) in the discussion of the faint-young-sun paradox: geothermal heating induced by the tidal deformation of the Earth by the newly formed Moon. In comparison to the other mechanisms detailed above, tidal heating always has a warming effect, whereas changes in the Earth's atmospheric composition, cloud coverage, land-to-surface fraction, albedo etc. could in principle also yield even lower temperatures in the absence of empirical model constraints. The energy budget difference between the initial and modern states of the Earth-Moon system provide firm constraints on the total amount of heat that must have been dissipated. Here we present the basic calculations to address this tidal energy budget.

2 Earth surface temperature

2.1 Sources of energy on the early Earth

The surface temperature of the early Earth was determined by a balance between the energy flux provided by different energy sources and the energy loss through radiation as infrared emission into space. The most important energy sources were absorption of the solar radiation, the translation of the kinetic energy of accreted material (planetesimals) into heat, radiogenic decay of short-lived isotopes in the Earth's mantle and crust, and, to a smaller amount, conversion of gravitational energy into heat during chemical stratification.

The solar radiation varied substantially during the first ∼50 Myr after the formation of the Sun (see Sect. 3). After the Moon-forming impact some 69 (±10) Myr after the beginning of the solar system (Maltese and Mezger, 2020), however, the solar flux settled at about 70 % of its modern value and then increased at a rate of about 6 % per billion years. The accretion of the Earth converted the gravitational energy of the incoming debris into heat on a time scale of 10 Myr to 100 Myr, the total amount of which was comparable to the solar heat absorbed at the time (Turcotte and Pflugrath, 1985). The most important short-lived radionuclides were ^{26}Al and ^{60}Fe (Urey, 1955; Chaussidon and Gounelle, 2007). Their short half life times of 0.7 Myr and 1.5 Myr, respectively, made them important sources of energy for the first 10 Myr or so, but negligible afterwards. The radiogenic decay of long-lived isotopes ^{40}K, ^{232}Th, ^{235}U, and ^{238}U provided about 0.2 W m^{-2} (Spohn, 1991; Gaidos et al., 2005) to the Hadean Earth. For comparison, the modern mean surface output of ^{238}U and ^{232}Th radioactive decay is $0.022^{+0.015}_{-0.010}$ W m^{-2} (Shimizu, 2015) and the global mean heat flow is 0.092 (± 0.004) W/m^2 (Davies and Davies, 2010), the residual heat being mostly due to cooling of the Earth from its accretion.

The Moon might have played another important role in the early Earth's energy budget. The key physical effect here is tidal heating, a phenomenon that is well known from observations of some of the rocky and icy moons of the solar system giant planets. Io, the innermost of the four big moons of Jupiter, for example, is the volcanically most active body in the solar system (Smith et al., 1979) and its primary source of internal energy is tidal heating, that is, strictly speaking the source of the internal heat is actually external. Orbital perturbations from the other major satellites around Jupiter force Io on an eccentric orbit (Peale et al., 1979). Io's global mean tidal energy flux is about 2 W m^{-2} (Spencer et al., 2000). Another prominent example is Saturn's moon Enceladus, which shows tidally driven cryovolcanism (Porco et al., 2006). Similar to the case of Io, the cause of the ongoing tidal heating in Enceladus is its forced orbital eccentricity. The ultimate circularization of its orbit is inhibited by its gravitational interaction with another neighboring moon, in this case of Saturn's moon Dione (Meyer and Wisdom, 2007).

Although detailed modeling of the tides in the Hadean Earth-Moon system cannot be found in the literature, the nearby Moon must have strongly deformed the Earth from its equilibrium shape. The fast rotation of the Earth compared to the orbital motion of the Moon led to a time lag (or a phase lag; Greenberg, 2009; Efroimsky and Makarov, 2013) between the line connecting the two centers of mass and the instantaneous orientation of the tidal bulge on Earth. This offset then led to friction inside the Earth, which triggered the tidal heating. Previous studies estimated that the contribution of tidal heating on the Earth's surface was $\lesssim$ 0.1 W m^{-2} about 100 Myr after the Moon-forming impact, and therefore irrelevant for the long term global energy budget (Zahnle et al., 2007). These estimates were based on a specific tidal model (the constant phase lag tidal model) (Darwin, 1879, 1880; MacDonald, 1964; Ferraz-Mello et al., 2008) that implies a homogeneous composition of the Earth and a specific parameterization of the Earth's tidal dissipation, technically speaking the second degree tidal Love number (k_2) (Love, 1909, 1911) and the tidal dissipation constant (Q) (Goldreich and Soter, 1966). Here we show that the tidal heating rates in the early Earth might have been higher than previously thought.

2.2 Energy balance in a gray atmosphere model

We start our calculations by addressing the fact that the Earth's global mean effective surface temperature (T_s) is given by the thermal equilibrium between the absorbed incoming solar radiation and other internal energy sources on the one hand, and the emitted infrared radiation on the other hand. With F_em as the emitted energy flux from Earth per unit surface area, we have (Stefan, 1879; Boltzmann, 1884; Planck, 1901)

$$T_{\mathrm{s}} = \left(\frac{F_{\mathrm{em}}}{\sigma_{\mathrm{SB}}} \right)^{1/4} \ , \tag{1}$$

where $\sigma_{\mathrm{SB}} = 5.670 \times 10^{-8}\,\mathrm{W\,m^{-2}\,K^{-4}}$ is the Stefan-Boltzmann constant. In modern Earth, F_{em} is dominated by the re-emission of the absorbed insolation,

$$F_{\mathrm{em}} = \frac{L_{\odot}(t)}{4\pi \mathrm{AU}^2} \frac{(1-\alpha)\epsilon}{f} \left(1 + \frac{3}{4}\tau \right) \ , \tag{2}$$

where $L_{\odot}$ is the time-dependent solar luminosity (t is time), ϵ is the Earth's emissivity[2], α is the Earth's Bond albedo, f is an energy redistribution factor that accounts for the Earth's rotation, AU = 150 million km is the Sun-Earth distance, and τ is the atmospheric infrared gray opacity (Feulner, 2012). In this equation, the Earth's atmosphere is assumed to be gray (Emden, 1913), that is, its radiative properties are independent of wavelength (λ). This approximation neglects the strong λ variability of the solar flux reflection, absorption, and re-emission by the various atmospheric gaseous components, dust, and clouds (Sagan, 1969; Wei et al., 2019). The term "gray" does not refer to the color of the atmosphere but to the non-dependence of the model on the wavelength.

For modern Earth, a typical parameterization of Eq. (2) uses $\alpha = 0.3$ and $f = 4$ (Selsis et al., 2007). Moreover, the gray opacity in the visible regime of the electromagnetic spectrum (called the optical depth) has been measured at the Earth's surface as $\tau \sim 0.35$ (Terez and Terez, 2003). For now, we take this value as a proxy for τ, which is assumed to be independent of wavelength, in the infrared but we rectify this assumption in Sect. 5 and calibrate τ with the observed greenhouse warming. The Earth's emissivity can be approximated as $\epsilon = 0.95$, between the values for water (0.96) and limestone (0.92). For modern values of the solar luminosity Eq. (2) yields $T = -6.3°\mathrm{C}$. The deviation of 20.3°C from the actual value of +14°C is due to the well-known λ dependence of the atmospheric greenhouse effect – mostly due to $\mathrm{H_2O}$, $\mathrm{CO_2}$, and $\mathrm{CH_4}$ – that is encapsulated in τ. Obviously, the optical depth is not a good proxy for the infrared gray opacity and we return to this aspect in Sect. 3 and Fig. 3. Nevertheless, Eq. (2) is a much better approximation than that of an airless Earth, which has a theoretical global mean equilibrium temperature of −18°C.

Early in the Earth's history, during as much as the first 1 Gyr after formation, the solar luminosity was only about 70 % of its current value, for which Eqs. (1) and (2) predict $T_{\mathrm{s}} = -29.1°\mathrm{C}$. Even additional heating from a greenhouse effect of about +20.3°C, as observed today, would be insufficient by far to prevent global freezing of the early Earth. More complex models that include both a warming greenhouse effect and an ice-albedo effect, which dramatically cools the planet as soon as it starts to have ice sheets, suggests that the Earth should have been even much cooler, raising the question of the yet unsolved early-faint-sun or faint-young-sun paradox (Sagan and Chyba, 1997). That said, the composition of the early Earth atmosphere was entirely different from its modern counterpart and significant amounts of $\mathrm{CO_2}$, $\mathrm{CH_4}$, and $\mathrm{NH_3}$ could have further raised surface temperatures by several degrees Celsius. Nonetheless, atmospheric effects alone

---

[2] Emissivity describes ratio of the thermal radiation from a surface of a given temperature compared to the radiation from a black body surface at the same temperature.

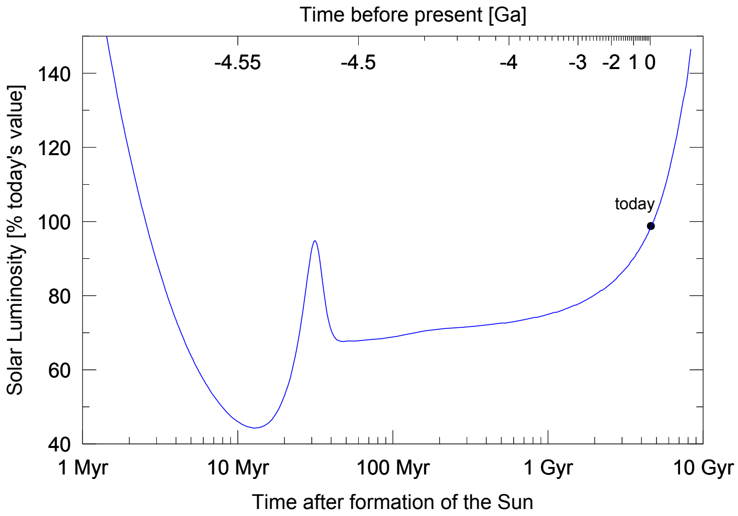

Fig. 2 Evolution of the solar luminosity as computed from a stellar evolution model (Baraffe et al., 2015). The age of the Sun of about 4.567 Gyr is labeled with a black dot, at which time the model predicts a luminosity of 98 % of the actual observed value. The abscissa at the bottom shows the modeled time after formation of the Sun-like star. The abscissa at the top shows the time before present in units of gigayears ago (Ga).

are unable to solve the faint-young-sun paradox (Kasting et al., 1988; Sagan and Chyba, 1997).

In the following, we use theoretical models to investigate the possible role of tidal heating in the Hadean and Archean Earth due to the young, nearby Moon. We use sedimentological and geochemical evidence for the presence of liquid water as benchmarks (see Sect. 1).

3 Evolution of the solar luminosity

Since the beginning, the energy budget of the Earth has been inherently liked with the luminosity of the Sun. The solar luminosity describes the electromagnetic energy output across all wavelengths and it currently amounts to 3.85×10^{26} W (Chapman, 1997) with decadal fluctuations of the order of 0.1 % (Solanki et al., 2013). The solar luminosity cannot reliably be reconstructed even on a level of 1 % for more than the past few decades. Hence, we resort to stellar evolution models to reconstruct $L_\odot(t)$ throughout the Earth's history.

Figure 2 shows a pre-computed stellar evolution model of a Sun-like star (Baraffe et al., 2015). The track illustrates the initial settling of the Sun on the main sequence, a phase which is dominated by radial shrinking and conversion of potential energy into heat. After about 20 Myr, the proton-proton nuclear reaction chain (Bethe, 1939) kicks in, upon which the Sun almost doubles its energy output. After ongoing shrinking until about 40 Myr into the life of the Sun, its luminosity settles at about 70 % of its modern value and then increases at a rate of a little less than 1 % per 100 Myr for the next Gyr. At the current age of the Sun, marked by a black dot at 4.567 Gyr along the bottom abscissa, the model predicts 98 %

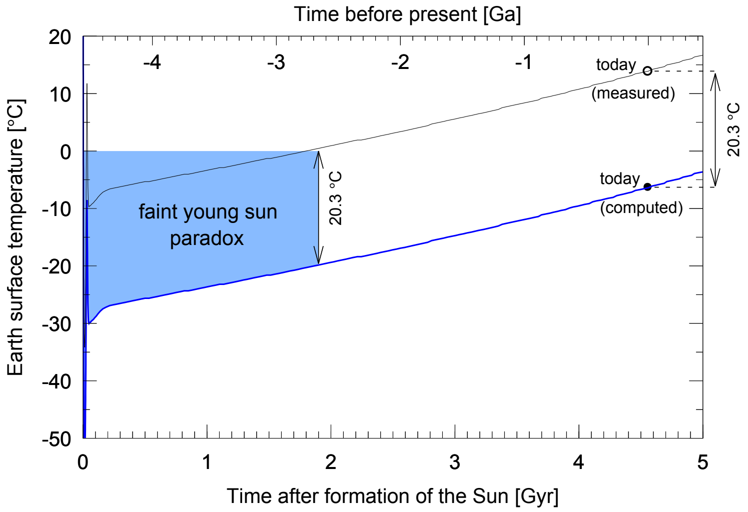

Fig. 3 Evolution of the early Earth's mean surface temperature under the assumption of a gray atmosphere, in which the wavelength dependence of the absorption of sunlight and re-emission in the infrared is neglected. The blue solid line shows results as per Eqs. (1)-(2) with $\tau = 0.35$ and using stellar evolution models (Baraffe et al., 2015). These models are multiplied by a factor of 1.02 to account for the offset between the predicted and the observed solar luminosity. The surface temperature computed for today is $-6.3°$C. The thin black line shows a model forced to fit the measured value of 14°C, for which $\tau = 0.925$ is required. The blue shaded area highlights the phase of sub-zero degree temperatures that cannot be explained by the additional heating of +20.3°C from a greenhouse effect as on modern Earth.

of the actual value of the solar power output. In the following, we compensate for this offset by multiplying the stellar evolution model by a factor of 1.02, which acts as a calibration to reproduce today's insolation.[3]

In Fig. 3 we illustrate the resulting evolution of the Earth's global mean effective surface temperature as per Eqs. (1) and (2). Different from Fig. 2, which uses a logarithmic scaling along the abscissa to highlight the strong luminosity variations of the young Sun, Fig. 3 uses a linear scaling. The blue shaded area, present until 1.9 Gyr after formation of the Sun (~ 2.7 Ga and before), marks the era of the early Earth, in which an additional heating of +20.3°C by a modern Earth-like greenhouse effect cannot prevent the early Earth from becoming a global snowball. This time scale agrees with previous estimates (Sagan and Chyba, 1997). The minimum temperatures achieved in this model are as low as nearly $-50°$C before the Sun reaches an age of 50 Myr. In extreme scenarios, additional greenhouse warming from CO_2, CH_4, and NH_3 could have prevented the late phase of the faint-young-sun paradox near 2.2 Gyr after formation of the Sun but not the first 700 Myr (about 3.9 Ga and before) with T_s as low as $-30°$C as predicted by the gray atmosphere model. The black line in Fig. 3 is obtained by using $\tau = 0.925$,

---

[3] Not shown in Fig. 2 is the variation of the solar spectral energy distribution, which might also have had a significant effect on the evolution of the Earth's atmospheric chemistry and therefore on the climate. To give just one example, the high-energy (short-wavelength, $\lambda <$ 100 nm) radiation of the early Sun (~4 Ga and before) was about 100 to 1000 times stronger than it is today (Ribas et al., 2005; Shapiro et al., 2020).

which raises temperatures by 20.3° and reproduces the global mean surface temperature on the modern Earth.

4 Tidal evolution

4.1 Mechanical energy loss through tides

The effect of tidal heating – caused by the tidal forces from the young and nearby Moon, which probably formed as close as about $3.8\,R_\oplus$ (Canup, 2004) following a giant impact 69 (±10) Myr after the beginning of the solar system (Maltese and Mezger, 2020) – on the climate of the early Earth has hitherto not been studied in detail (but see Blackledge et al. 2020 for tidal simulations of Archean-like conditions in the Earth-Moon system). It has been suggested that tidal heating in the Earth has dropped below $100\,\mathrm{W\,m^{-2}}$ within a few Myr after the Moon forming event and below $0.1\,\mathrm{W\,m^{-2}}$ within 100 Myr (Zahnle et al., 2007). These estimates were based on parameterized models of tidal equilibrium theory with a fixed second order tidal Love number (k_2) and constant tidal dissipation factor (Q) for the Earth. It is well-known, however, that the tidal dissipation of viscous objects, such as the partly molten early Earth, is strongly dependent on the frequency of the tide-raising potential (Greenberg, 2009), i.e. the Keplerian orbital frequency of the Moon in the reference frame rotating with the Earth. The feedback mechanism between the warming effect of tidal heating on the melt fraction of the early Earth's mantle and the resulting change of the efficiency of tidal heating, which have been studied for extrasolar Earth-like planets (Henning et al., 2009; Henning and Hurford, 2014), have also not been studied in the young Earth-Moon system so far.

We do not consider these feedback mechanisms or the frequency dependence of the tidal Q factor in this report either. Instead, our point is that previous calculations underestimated the effect of the enormous transfer of angular momentum from the fast-spinning early Earth to the orbit of the Moon (and the concomitant strong tidal heating) after the Moon-forming impact. In principle, this mechanism has been known for a long time, both from theory (Webb, 1980, 1982) and from the interpretation of a banded iron formation in Australia (Walker and Zahnle, 1986). Only recent advances in computer simulations of the actual impact scenario, however, suggested that the post-impact Earth had an extremely short rotation period, possibly near 2.2 hr (Canup, 2012), which is several times faster than previously assumed. As we demonstrate below, the resulting total amount of the dissipated tidal energy could have had a significant effect on the early Earth's energy budget.

To set the stage for our tidal heating calculations, we compute the total rotational and orbital energy in the Earth-Moon system directly after formation and today. Since the Earth-Moon system does not lose significant portions of its mechanical energy through other mechanisms than tidal dissipation, we can safely assume that the difference between the modern and early state of the system has been dissipated through tides almost exclusively inside the Earth.[4] We assume that both the Earth and the Moon are solid, homogeneous spheres with masses

---

[4] Tides raised on the Earth by the Sun also contribute to the energy dissipation in the Earth's rotation, but solar tides were only on a percent level since the formation of the Earth-Moon system (Canup et al., 2001).

of $M_\oplus = 5.9736 \times 10^{24}$ kg and $M_☾ = 7.3477 \times 10^{22}$ kg and with radii of $R_\oplus = 6378$ km and $R_☾ = 1737$ km, respectively. Generally, the rotational energy of a solid sphere is $E_\mathrm{rot} = 1/2\, I\omega^2$, where $I = 2/5\, MR^2$ is the moment of inertia of a sphere with mass M and radius R, and $\omega = v_\mathrm{rot}/R$ is the angular velocity. The equatorial rotational speed $v_\mathrm{rot} = 2\pi R/P_\mathrm{rot}$ can be calculated using the rotational period P_rot. As a consequence,

$$E_\mathrm{rot} = \frac{1}{5} M \left(\frac{2\pi R}{P_\mathrm{rot}} \right)^2 . \tag{3}$$

In addition to the rotational energy, there is orbital energy in the system, which is mostly stored in the orbital motion of the Moon, which is given as

$$E_{\mathrm{orb},☾} = \frac{1}{2} M_☾ \left(\frac{2\pi a}{P_\mathrm{orb}} \right)^2 , \tag{4}$$

where a is the Moon's orbital semimajor axis on its Keplerian orbit around the Earth and $P_\mathrm{orb} = 2\pi\sqrt{a^3/(G(M_\oplus + M_☾))}$ is its orbital period, as stated by Newton's derivation of Kepler's third law of motion (Kepler et al., 1619). For the initial post-impact state of the system we use $a' = 3.8\, R_\oplus$, which gives $P'_\mathrm{orb} = 10.4$ hr.[5] Today, $a = 60.3\, R_\oplus$ and $P_\mathrm{orb} = 27.32$ d. The total energy of the early Earth-Moon system and of the modern Earth-Moon system then is

$$E'_\mathrm{tot} = E'_{\mathrm{rot},\oplus} + E'_{\mathrm{rot},☾} + E'_{\mathrm{orb},☾} = 3.12 \times 10^{31}\ \mathrm{J} \tag{5}$$

$$E_\mathrm{tot} = E_{\mathrm{rot},\oplus} + E_{\mathrm{rot},☾} + E_{\mathrm{orb},☾} = 3.11 \times 10^{29}\ \mathrm{J} . \tag{6}$$

In other words, the amount of mechanical energy stored in the modern Earth-Moon system is about 1 % of the initial amount. 99 % of the initial amount of mechanical energy has been dissipated as heat through the Earth's surface in its 4.5 Gyr history. This amount of energy is comparable to the modern solar energy output within one day.

4.2 Tidal heating

The tidal evolution of the Earth-Moon system has initially been described in a rigorous mathematical framework by G. H. Darwin (Darwin, 1880), who developed an equilibrium tide model. This model assumes that the gravitational force of the tide raiser (here the Moon) elongates the perturbed body (here the Earth) and that this distortion is slightly misaligned to the line connecting the two centers of mass. This misalignment is due to dissipative processes within the deformed body, that is, currently mostly in the Earth's oceans, and it leads to a secular evolution of the orbit and spin angular momenta (Zschau, 1978).

The constant-phase-lag model assumes that the phase (or angle) lag between the Earth's equilibrium tidal bulge and the line connecting the Earth-Moon barycenters is constant during the orbit (Ferraz-Mello et al., 2008; Greenberg, 2009; Heller

---

[5] Here and in the following, quantities referring to the early Earth-Moon system are labeled with a prime (′).

et al., 2011; Efroimsky and Makarov, 2013). In the limit of small orbital eccentricities and spin-orbit misalignments we can estimate the tidal heating in the Earth due to its tidally induced spin-down owing to the Moon:

$$\dot{E}_{\rm tid} = \frac{3}{2}\, G^2\, k_{\rm d,\oplus}\, M_{☾}^2\, (M_\oplus + M_{☾})\, \frac{R_\oplus^5}{a^9}\, \frac{1}{nQ_\oplus} \varepsilon_{0,\oplus} \left(\frac{\omega_\oplus}{n} - 1\right) \tag{7}$$

where G is the gravitational constant, $k_{\rm d,\oplus} = 0.3$ the Earth's second-degree tidal Love number, $n = 2\pi/P$ the orbital frequency, $\omega_\oplus = 2\pi/P_\oplus$ the Earth's rotational frequency, $\varepsilon_{0,\oplus} = 2\omega_\oplus - 2n$ the tidal frequency, and where $Q'_\oplus$ is the Earth's tidal dissipation constant. Knowing that $n = \sqrt{G(M_\oplus + M_{☾})}a^{-3/2}$, as per Kepler's 3rd law of motion, one can show that Eq. (7) implies

$$\dot{E}_{\rm tid} \propto r^{-6} \quad \text{for } L_{\rm tot} \gg L_{\rm orb} \text{ (in the early phase),} \tag{8}$$

$$\dot{E}_{\rm tid} \propto r^{-5.5} \quad \text{for } L_{\rm tot} \approx L_{\rm orb} \text{ (nowadays).} \tag{9}$$

The current value of $Q_\oplus \approx 10$ is relatively low compared to the other rocky objects in the solar system, for which it is mostly around 100 (Goldreich and Soter, 1966). The low $Q_\oplus$ value likely results from its strong dependence on the tidal frequency and from the fact that it is currently dominated by dissipation in the shallow waters of the Earth oceans (Webb, 1980, 1982). These tidal forcing properties of the Earth change over time as the continents (and oceans) drift. Assuming a conservative value of $Q'_\oplus = 100$ (or today's value of $Q'_\oplus = 10$), this yields

$$\dot{E}'_{\rm tid}(Q'_\oplus = 10) = 52\,{\rm W\,m^{-2}}, \tag{10}$$

$$\dot{E}'_{\rm tid}(Q'_\oplus = 100) = 5.2\,{\rm W\,m^{-2}}, \tag{11}$$

for the early Earth or, more generally,

$$\dot{E}'_{\rm tid} = 52\,{\rm W\,m^{-2}} \left(\frac{10}{Q'_\oplus}\right) \left(\frac{3.8\,R_\oplus}{r'}\right)^6 . \tag{12}$$

This approximation neglects additional tidal heating from the tidal circularization of an eccentric orbit as well as the tidally induced spin-orbit alignment (Heller et al., 2011). As an aside, in the absence of significant eccentricity or obliquity, Barnes (2017) finds that $Q_\oplus = 34.5$ results in an orbital evolution that places the Moon at the Earth's surface 4.5 Ga. Although the Moon did not form at the Earth's surface but near the Earth's Roche radius, beyond which tidal forces were too weak to prevent accretion of the Moon, this proxy results in initial tidal heating rates near 15 W m^{-2}. For comparison, three-dimensional simulations of tidal dissipation in the early Earth oceans suggest that $Q_\oplus \sim 1$ might, under certain circumstances, be plausible (Blackledge et al., 2020). The corresponding tidal heating rates would be 520 W m^{-2} according to Eq. (12).

The resulting transfer of angular momentum between the Earth's rotation and the orbit of the Moon leads to an increase of a and, hence, to a decrease of $\dot{E}'_{\rm tid}$ on a time scale of 10 Myr to 100 Myr, the details of which are in fact unknown. Detailed modeling of the tidal heating evolution in the early Earth would require

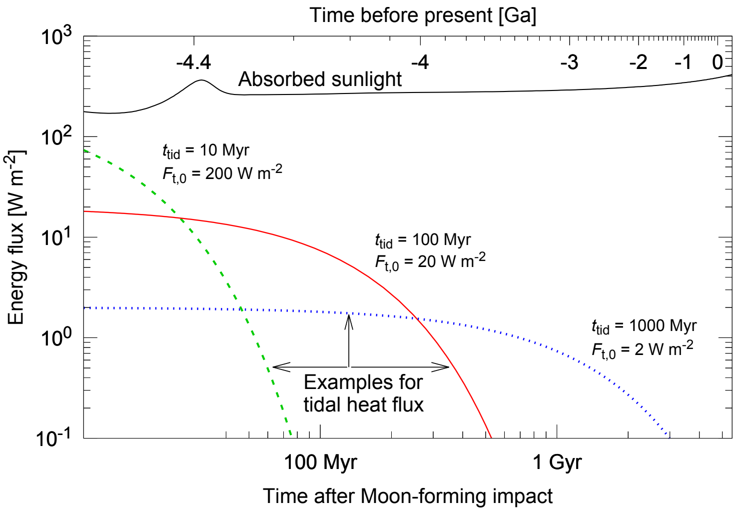

Fig. 4 Calculated tidal heat flux in the early Earth compared to the absorbed radiation from the young Sun (black solid line). Three different choices of the parameterization of Eq. (13) result in the example tidal heat fluxes as labeled along the tracks.

a better knowledge of the planetary structure, in particular of the thickness and temperature of a possible mantle in which most of the tidal heating is supposed to occur (Henning et al., 2009). Our knowledge of the internal evolution of the early Earth after the Moon forming giant impact, however, is far from being complete. In fact, these uncertainties in the parameterization of the model would dominate the (unknown and so far untestable) errors in the results of a detailed modeling of the orbital evolution in the early Earth-Moon system.

Because of these uncertainties, we choose a much more simple but not necessarily much less plausible approach and characterize the evolution of the tidal heating rate by a characteristic tidal heat flux ($F_{\mathrm{t},0}$), which Eq. (12) suggests to be about 52 W m^{-2} in the early Earth, and a characteristic time scale for the tidal evolution (t_{tid}). Orbital evolution due to tides as well as the resulting tidal heating often follow an exponential or near-exponential decay law (Zahnle et al., 2007). We therefore parameterize the evolution of the tidal heat flux as

$$F_{\mathrm{t}}(t) = F_{\mathrm{t},0}\, e^{-t/t_{\mathrm{tid}}} \ . \tag{13}$$

As a boundary condition for Eq. (13) the tidal surface heat flux integrated over the age the Earth (T) and multiplied by the surface of the Earth must be equal to the difference between the amounts of mechanical energy in the early and modern Earth-Moon systems (Eqs. 5-6),

$$4\pi R_{\oplus}^2 \int\limits_0^T \mathrm{d}t \ F_{\mathrm{t}}(t) = E'_{\mathrm{tot}} - E_{\mathrm{tot}} \ = \ 3.09 \times 10^{31}\,\mathrm{J} \ . \tag{14}$$

In Fig. 4 we show the tidal heat flux in the early Earth for three different choices of t_{tid} and $F_{\mathrm{t},0}$ in Eq. (13) that satisfy Eq. (14). All three choices are compared to the absorbed electromagnetic energy flux from the Sun as per Eqs. (1) and (2) and using pre-computed stellar evolution models (Baraffe et al., 2015) (black solid line). We find that even the most extreme parameterization of the tidal heat flux with $t_{\mathrm{tid}} = 10\,\mathrm{Myr}$ and $F_{\mathrm{t},0} = 200\,\mathrm{W\,m^{-2}}$ (green dashed line) can barely compete with the solar absorbed flux on a time scale of 10 Myr, a time which would be measured after the Moon-forming impact. A more moderate and more reasonable choice of $t_{\mathrm{tid}} = 100\,\mathrm{Myr}$ and $F_{\mathrm{t},0} = 20\,\mathrm{W\,m^{-2}}$ (red solid line) results in about $10\,\mathrm{W\,m^{-2}}$ of tidal surface heating for the first ∼100 Myr after formation of the Earth and therefore could have been a significant source of energy during its early lifetime. This parameterization is used again as a reference tidal heat flux in Fig. 5. The resulting decay of tidal heating is in agreement with previous estimates (Feulner, 2012) of $\sim\ 0.02\,\mathrm{W\,m^{-2}}$ during the Archean (4 Ga-2.5 Ga). An even more moderate parameterization using $t_{\mathrm{tid}} = 1000\,\mathrm{Myr}$ and $F_{\mathrm{t},0} = 2\,\mathrm{W\,m^{-2}}$ (blue dotted line) would keep tidal heating about two orders of magnitude smaller than the amount of absorbed sunlight.

Although any plausible parameterization produces a tidal heat flux that is small compared to the solar energy input, even a conservative value of $F_{\mathrm{t},0} = 2\,\mathrm{W\,m^{-2}}$ is comparable to the global mean flux from tidal heating observed on Jupiter's volcanically active moon Io (Spencer et al., 2000). It has been argued that this level of a surface heating through an internal heat source could trigger global volcanism on Earth-sized planets as well (Barnes et al., 2009). If this were the case, then even our most conservative choice of the parameterization of the evolution of tidal heating could have resulted in extreme geophysical processes on the early Earth that could possibly have produced strong enhanced CO_2 outgassing and a substantial, long lasting greenhouse effect. In other words, beyond the direct heating effect of tidal friction, tides could have triggered further geophysical activities, which – as a secondary effect – could have heated the early Earth. Beyond that, the rapid resurfacing could have precluded the development of a biosphere (Barnes et al., 2009).

The comparison with the global mean internal heat emission of $2\,\mathrm{W\,m^{-2}}$ from the surface of the volcanically active Io introduces another interesting possibility. The widespread occurrence of ultramafic rocks such as komatiites before 3 Ga has been interpreted as evidence for a higher geothermal gradient in the early Earth (Nesbitt et al., 1982; Herzberg et al., 2010). A detailed study of the convective heat and matter transport in the early Earth's mantle and crust are beyond the scope of this article. However, our results demonstrate the potential of tidal heating as a mechanism to explain, at least partly, the observations of two phenomena, that is, the faint-young-sun paradox and the enhanced internal heat flow in the Archean.

On the more speculative side, the tidal forces acting on the crust of the Archean Earth might have left scars in the geological record. The thousands of black chert veins mapped in the North Pole region in Western Australia (see Fig 1a,b) demonstrate intensive brittle deformation of the oceanic crust 3.49 Ga. Part of the Dresser Formation is also a caldera structure (van Kranendonk et al., 2008) and some part of the veins could be formed via this collapse structure. The majority of them, however, must have an alternative origin and the strong tidal forces caused by the nearby early Moon might have played a role. Fractures with carbonate infilling observed in the 3.47 Gyr old Mt. Ada Basalt (see Fig 1c) serve as another piece of evidence of brittle deformation in cooled oceanic crust and enhanced geothermal activity in the Archean Earth.

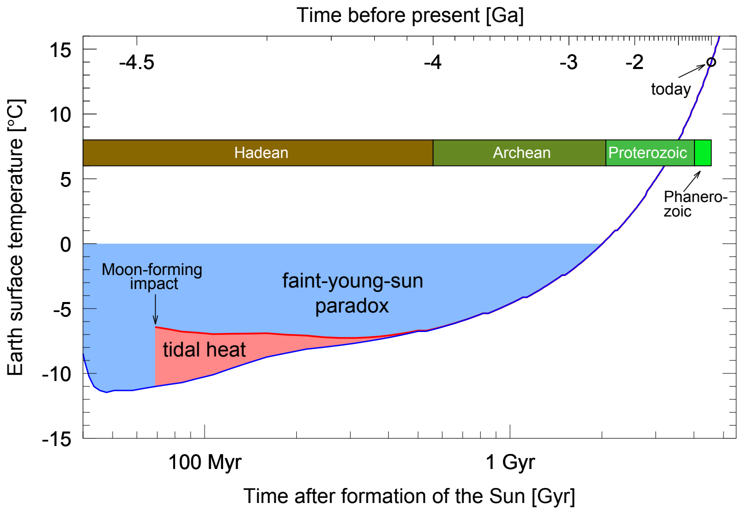

Fig. 5 Evolution of the early Earth's mean surface temperature using energy input from both insolation and tidal heat flux. The gray opacity of the Earth atmosphere is set to $\tau = 0.925$ to force the atmosphere model to reproduce modern Earth temperatures. The blue line shows results as per Eqs. (1) and (2) and using stellar evolution models (Baraffe et al., 2015) calibrated to reproduce the modern power output of the Sun. The blue shaded area highlights the phase of sub-zero temperatures. The red shaded area, the integral of which contains 3.09×10^{31} J as per Eq. (14), illustrates an increase of the temperature due to tidal heating assuming $F_{\mathrm{t},0} = 20\,\mathrm{W\,m^{-2}}$ and $t_{\mathrm{tid}} = 100$ Myr in Eq. (13). Geological ages are highlighted with horizontal bars. In summary, tidal heating alone cannot possibly solve the faint-young-sun paradox. Nevertheless, it could have been an important ($> 1^\circ$C) compensation of the low solar luminosity in the first ~ 220 Myr (before about 4.35 Ga) to prevent a global snowball Earth.

5 Combination of solar luminosity and tidal heating

Equipped with Eq. (2) for the globally averaged insolation absorbed by the Earth, a pre-computed track of the solar luminosity to feed into Eq. (2), and an evolutionary model for the Earth's tidal heat flux as per Eq. (13), we can now set $F_{\mathrm{em}} = F_\odot + F_{\mathrm{t}}$ in Eq. (1) and re-evaluate the evolution of the Earth's global mean surface temperature.

We calibrate Eq. (2) to reproduce the modern Earth value of $T_{\mathrm{s}} = +14^\circ\mathrm{C}$ by setting the infrared gray opacity to $\tau = 0.925$. This approach can be seen as forcing the gray atmosphere model to encapsulate all the complex radiative properties of the Earth's atmospheric gases in the free parameter τ. We also choose $F_{\mathrm{t},0} = 20\,\mathrm{W\,m^{-2}}$ and $t_{\mathrm{tid}} = 100$ Myr in Eq. (13), a parameterization that gives a total amount of dissipated tidal energy through the Earth's surface that is compatible with the observations from orbital mechanics (Eqs. 5-6).

In Fig. 5 we plot $T_{\mathrm{s}}(t)$ for this parameterization of the model. The blue line at the bottom refers to the gray atmosphere model (forced to reproduce modern Earth surface temperatures) without the additional contribution of tidal heating. The minimum temperatures reached in this model are -11.5°C at 50 Myr after formation of the Sun.

The red line in Fig. 5 refers to Earth's mean surface temperature based on the sum of the tidal plus solar absorbed flux on Earth. The contribution from tidal heating on the early Earth's surface temperature is highlighted by the red shaded area. In this model, the Moon-forming impact (set to 69 Myr after the formation of the Sun; Maltese and Mezger, 2020) results in an addition of tidal heat flux, which keeps temperatures near -7°C instead of the -11.5°C mentioned above. In the following, the tidal heat flux decreases while the solar luminosity increases by comparable fraction. As a consequence, the Earth's surface temperature remains almost constant near -7°C. After this phase, tidal heating vanishes, whereas the solar luminosity continues to climb. The temperature offset triggered by tidal heating is up to about $+5^\circ$C within the first 10 Myr after the Moon-forming impact and $> 1^\circ$C for the first $\sim$ 150 Myr of the newly formed Earth-Moon system. Assuming a Moon-forming impact 69 Myr after formation of the Sun, our results imply that tidal heating could have been significant for the maintenance of liquid surface water up until ∼220 Myr after the formation of the Sun, that is, until about 4.35 Ga (see Fig. 5). The periods of the Hadean (4.56 Ga–4 Ga), Archean (4 Ga–2.5 Ga), Proterozoic (2.5 Ga–541 Ma), and Phanerozoic (541 Ma–today) geological ages are also shown in Fig. 5. This comparison shows that tidal heating in the Earth due to the nearby Moon was only relevant in the Hadean, at least for this choice of a paramterization of our model.

We have also explored other reasonable parameterizations of Eq. (13) and found that, in no case, tidal heating alone could contribute the required amount of heat to bypass the faint-young-sun paradox and prevent a global snowball Earth. Either tidal heating is short ($t_{\rm tid} \lesssim 10$ Myr) and extreme ($F_{\rm t,0} \sim 200\,{\rm W\,m^{-2}}$). In this case it is sufficiently strong to push the global mean temperature of the early Earth above 0°C – but only for a few Myr and therefore much too short. Alternatively, tidal heating acts on a longer time scale ($t_{\rm tid} \gtrsim 100$ Myr) and with a more moderate magnitude ($F_{\rm t,0} \sim 20\,{\rm W\,m^{-2}}$), but then it never lifts $T_{\rm s}$ above 0°C.

Irrespective of the details of the actual evolution of tidal heating, the overall dissipation of the mechanical energy budget (Sect. 4.2) suggests that this mechanism was not negligible in the early Earth. On the contrary, we demonstrate that tidal heating factored significantly into the heat budget of early Earth, likely contributing to the prevention of a global snowball state.

6 Conclusions

We have shown that the modern Earth-Moon system only contains about 1 % of its initial spin-orbit energy budget, when the Earth was a fast rotator and the Moon was in an extremely tight orbit. Most of the energy has been dissipated through tides, and we show that the resulting tidal heating may have had a much larger effect on the Earth's mean surface temperature than previously thought. Our combination of a gray atmosphere model with an *ad hoc* model for the evolution of the Earth's tidal heating rate, which is compatible with the total energy released in the Earth-Moon system, predicts that tidal heating may have contributed a heating of several degrees Celsius within the first ∼100 Myr of the life of the Earth.

Although tidal heating in the Earth from a nearby Moon cannot possibly solve the faint-young-sun paradox alone, our results suggest that it could have played an important role in maintaining liquid water at the surface. As a bonus, tidal heating as a geothermal heat source might have helped to sustain enhanced mantle temperatures, for instance by driving hydrothermal fluid circulation in early Earth's crust. This interpretation would be compatible with the previously stated "hydrothermal pump" concept, which asks for an internal heat source and strong forces in the crust of the Archean Earth to explain the presence of 3.49 Gyr old black chert veins of the Dresser Formation (Western Australia). A unified model that includes geophysical, atmospheric, tidal, and astrophysical effects could be able to resolve the longstanding faint-young-sun paradox.

Acknowledgements The authors are thankful to Rory Barnes for helpful comments on the manuscript.

Funding. RH is supported by the German space agency (Deutsches Zentrum für Luft- und Raumfahrt) under PLATO Data Center grant 50OO1501. JPD and JR acknowledge support from the DFG SPP 1833 "Building a Habitable Earth" (DU 1450/3-1, DU 1450/3-2, and RE 665/42-2).

Conflict of interest. The authors declare that they have no conflict of interest.

Availability of data and material. Not applicable.

Code availability. The `gnuplot` scripts used to plots Figs. 2-5 can be requested via e-mail from author RH (heller@mps.mpg.de).

References

Allwood AC, Walter MR, Kamber BS, Marshall CP, Burch IW (2006) Stromatolite reef from the early archaean era of australia. Nature 441(7094):714–718, DOI 10.1038/nature04764

Amelin Y, Krot A (2007) Pb isotopic age of the allende chondrules. Meteoritics & Planetary Science 42(7-8):1321–1335, DOI 10.1111/j.1945-5100.2007.tb00577.x

Arndt N (2011) Ga, Springer Berlin Heidelberg, Berlin, Heidelberg, pp 621–621. DOI 10.1007/978-3-642-11274-4_611

Baraffe I, Homeier D, Allard F, Chabrier G (2015) New evolutionary models for pre-main sequence and main sequence low-mass stars down to the hydrogen-burning limit. A&A 577:A42, DOI 10.1051/0004-6361/201425481

Barnes R (2017) Tidal locking of habitable exoplanets. Celestial Mechanics and Dynamical Astronomy 129(4):509–536, DOI 10.1007/s10569-017-9783-7, `1708.02981`

Barnes R, Jackson B, Greenberg R, Raymond SN (2009) Tidal Limits to Planetary Habitability. ApJL 700(1):L30–L33, DOI 10.1088/0004-637X/700/1/L30

Bethe HA (1939) Energy production in stars. Phys Rev 55:434–456, DOI 10.1103/PhysRev.55.434

Blackledge BW, Green JAM, Barnes R, Way MJ (2020) Tides on Other Earths: Implications for Exoplanet and Palaeo-Tidal Simulations. Geophys. Res. Lett.47(12):e85746, DOI 10.1029/2019GL085746

Boltzmann L (1884) Ableitung des Stefan'schen Gesetzes, betreffend die Abhängigkeit der Wärmestrahlung von der Temperatur aus der electromagnetischen Lichttheorie. Annalen der Physik 258(6):291–294, DOI 10.1002/andp.18842580616

von Brunn V, Gold D (1993) Diamictite in the archaean pongola sequence of southern africa. Journal of African Earth Sciences (and the Middle East) 16(3):367 – 374, DOI 10.1016/0899-5362(93)90056-V

Canup RM (2004) Simulations of a late lunar-forming impact. Icarus 168(2):433 – 456, DOI 10.1016/j.icarus.2003.09.028

Canup RM (2012) Forming a moon with an earth-like composition via a giant impact. Science 338(6110):1052–1055, DOI 10.1126/science.1226073

Canup RM, Ward WR, Cameron AGW (2001) A Scaling Relationship for Satellite-Forming Impacts. Icarus 150(2):288–296, DOI 10.1006/icar.2000.6581

Catling DC, Zahnle KJ (2020) The archean atmosphere. Science Advances 6(9), DOI 10.1126/sciadv.aax1420

Chapman GA (1997) Solar luminosity, Springer Netherlands, Dordrecht, pp 748–748. DOI 10.1007/1-4020-4520-4_374

Charnay B, Wolf ET, Marty B, Forget F (2020) Is the faint young Sun problem for Earth solved? arXiv e-prints: 2006.06265

Chaussidon M, Gounelle M (2007) Short-lived radioactive nuclides in meteorites and early solar system processes. Comptes Rendus Geoscience 339(14):872 – 884, DOI 10.1016/j.crte.2007.09.005, formation du système solaire : approche cosmochimique dans le conteste astrophysique

Darwin GH (1879) On the precession of a viscous spheroid and on the remote history of the Earth. Philosophical Transactions of the Royal Society 170:447–530, (repr. Scientific Papers, Cambridge, Vol. II, 1908)

Darwin GH (1880) On the Secular Changes in the Elements of the Orbit of a Satellite Revolving about a Tidally Distorted Planet. Royal Society of London Philosophical Transactions Series I 171:713–891

Davies JH, Davies DR (2010) Earth's surface heat flux. Solid Earth 1(1):5–24, DOI 10.5194/se-1-5-2010

Duda JP, van Kranendonk MJ, Thiel V, Ionescu D, Strauss H, Schäfer N, Reitner J (2016) A rare glimpse of paleoarchean life: Geobiology of an exceptionally preserved microbial mat facies from the 3.4 ga strelley pool formation, western australia. PLOS ONE 11(1):1–18, DOI 10.1371/journal.pone.0147629

Duda JP, Thiel V, Bauersachs T, Mißbach H, Reinhardt M, Schäfer N, Van Kranendonk MJ, Reitner J (2018) Ideas and perspectives: hydrothermally driven redistribution and sequestration of early archaean biomass – the "hydrothermal pump hypothesis". Biogeosciences 15(5):1535–1548, DOI 10.5194/bg-15-1535-2018

Efroimsky M, Makarov VV (2013) Tidal Friction and Tidal Lagging. Applicability Limitations of a Popular Formula for the Tidal Torque. ApJ764(1):26, DOI 10.1088/0004-637X/764/1/26, 1209.1615

Emden R (1913) Über Strahlungsgleichgewicht und atmosphärische Strahlung. Ein Beitrag zur Theorie der oberen Inversion. Sitzungsberichte der mathematisch-physikalischen Klasse der Bayerischen Akademie der Wissenschaften München (1):55–142

Ferraz-Mello S, Rodríguez A, Hussmann H (2008) Tidal friction in close-in satellites and exoplanets: The Darwin theory re-visited. Celestial Mechanics and Dynamical Astronomy 101:171–201, DOI 10.1007/s10569-008-9133-x

Feulner G (2012) The faint young Sun problem. Reviews of Geophysics 50(2):RG2006, DOI 10.1029/2011RG000375

Flament N, Coltice N, Rey PF (2008) A case for late-archaean continental emergence from thermal evolution models and hypsometry. Earth and Planetary Science Letters 275(3):326 – 336, DOI 10.1016/j.epsl.2008.08.029

Gaidos E, Deschenes B, Dundon L, Fagan K, Menviel-Hessler L, Moskovitz N, Workman M (2005) Beyond the Principle of Plentitude: A Review of Terrestrial Planet Habitability. Astrobiology 5:100–126, DOI 10.1089/ast.2005.5.100

Goldblatt C, Zahnle KJ (2011) Clouds and the faint young sun paradox. Climate of the Past 7(1):203–220, DOI 10.5194/cp-7-203-2011

Goldreich P, Soter S (1966) Q in the Solar System. Icarus 5(1):375–389, DOI 10.1016/0019-1035(66)90051-0

Greenberg R (2009) Frequency Dependence of Tidal q. ApJL 698(1):L42–L45, DOI 10.1088/0004-637X/698/1/L42

Haqq-Misra JD, Domagal-Goldman SD, Kasting PJ, Kasting JF (2008) A Revised, Hazy Methane Greenhouse for the Archean Earth. Astrobiology 8(6):1127–1137, DOI 10.1089/ast.2007.0197

Heller R, Leconte J, Barnes R (2011) Tidal obliquity evolution of potentially habitable planets. A&A 528:A27, DOI 10.1051/0004-6361/201015809

Henning WG, Hurford T (2014) Tidal Heating in Multilayered Terrestrial Exoplanets. ApJ 789(1):30, DOI 10.1088/0004-637X/789/1/30

Henning WG, O'Connell RJ, Sasselov DD (2009) Tidally Heated Terrestrial Exoplanets: Viscoelastic Response Models. ApJ 707:1000–1015, DOI 10.1088/0004-637X/707/2/1000

Herzberg C, Condie K, Korenaga J (2010) Thermal history of the earth and its petrological expression. Earth and Planetary Science Letters 292(1):79 – 88, DOI 10.1016/j.epsl.2010.01.022

Hickman AH (1977) New and revised definitions of rock units in the warrawoona group, pilbara block. Geological Survey of Western Australia, Annual Report 1976:58

Hickman-Lewis K, Cavalazzi B, Foucher F, Westall F (2018) Most ancient evidence for life in the barberton greenstone belt: Microbial mats and biofabrics of the ~3.47 ga middle marker horizon. Precambrian Research 312:45 – 67

Homann M (2019) Earliest life on earth: Evidence from the barberton greenstone belt, south africa. Earth-Science Reviews 196:102888

Kasting JF (1982) Stability of ammonia in the primitive terrestrial atmosphere. J Geophys Res 87(C4):3091–3098, DOI 10.1029/JC087iC04p03091

Kasting JF (1987) Theoretical constraints on oxygen and carbon dioxide concentrations in the precambrian atmosphere. Precambrian Research 34(3):205 – 229, DOI 10.1016/0301-9268(87)90001-5

Kasting JF, Siefert JL (2002) Life and the Evolution of Earth's Atmosphere. Science 296(5570):1066–1068, DOI 10.1126/science.1071184

Kasting JF, Toon OB, Pollack JB (1988) How climate evolved on the terrestrial planets. Scientific American 258:90–97, DOI 10.1038/scientificamerican0288-90

Kepler J, Ptolemaeus C, Fludd R (1619) Harmonices mvndi libri v. qvorvm primus geometricvs, de figurarum regularium, quae proportiones harmonicas constituunt, ortu & demonstrationibus, secundus architectonicvs, SEU EX geometria figvrata, de figurarum regularium congruentia in plano vel solido: tertius proprie harmonicvs, de proportionum harmonicarum ortu EX figuris

Knauth LP (2005) Temperature and salinity history of the precambrian ocean: implications for the course of microbial evolution. Palaeogeography, Palaeoclimatology, Palaeoecology 219(1):53 – 69, DOI https://doi.org/10.1016/j.palaeo.2004.10.014, URL http://www.sciencedirect.com/science/article/pii/S0031018204005905, geobiology: Objectives, Concept, Perspectives

van Kranendonk MJ (2011) Morphology as an indictor of biogenicity for 3.5–3.2 ga fossil stromatolites from the pilbara craton, western australia. In: J R, V QN, G A (eds) Advances in Stromatolite Geobiology, Springer Berlin Heidelberg, Berlin, p 32, DOI 10.1007/978-3-642-10415-2_32

van Kranendonk MJ, Philippot P, Lepot K, Bodorkos S, Pirajno F (2008) Geological setting of earth's oldest fossils in the ca. 3.5 ga dresser formation, pilbara craton, western australia. Precambrian Research 167(1):93 – 124, DOI 10.1016/j.precamres.2008.07.003

van Kranendonk MJ, Contributors:, Altermann W, Beard BL, Hoffman PF, Johnson CM, Kasting JF, Melezhik VA, Nutman AP, Papineau D, Pirajno F (2012) Chapter 16 - a chronostratigraphic division of the precambrian: Possibilities and challenges. In: Gradstein FM, Ogg JG, Schmitz MD, Ogg GM (eds) The Geologic Time Scale, Elsevier, Boston, pp 299 – 392

Kuhn WR, Atreya SK (1979) Ammonia photolysis and the greenhouse effect in the primordial atmosphere of the earth. Icarus 37(1):207–213, DOI 10.1016/0019-1035(79)90126-X

Kuhn WR, Kasting JF (1983) Effects of increased CO2 concentrations on surface temperature of the early earth. Nature 301:53–55, DOI 10.1038/301053a0

Liu Lg (2004) The inception of the oceans and co2-atmosphere in the early history of the earth. Earth and Planetary Science Letters 227(3-4):179–184, DOI 10.1016/j.epsl.2004.09.006

Love AEH (1909) The Yielding of the Earth to Disturbing Forces. Proceedings of the Royal Society of London Series A 82(551):73–88, DOI 10.1098/rspa.1909.0008

Love AEH (1911) Some Problems of Geodynamics

Lowe DR (1980) Stromatolites 3,400-myr old from the archean of western australia. Nature 284(5755):441–443, DOI 10.1038/284441a0

MacDonald GJF (1964) Tidal friction. Reviews of Geophysics 2(3):467–541, DOI 10.1029/RG002i003p00467

Maltese A, Mezger K (2020) The pb isotope evolution of bulk silicate earth: Constraints from its accretion and early differentiation history. Geochimica et Cosmochimica Acta 271:179 – 193, DOI 10.1016/j.gca.2019.12.021

Meyer J, Wisdom J (2007) Tidal heating in enceladus. Icarus 188(2):535 – 539, DOI 10.1016/j.icarus.2007.03.001

Miller SL, Urey HC (1959) Organic Compound Synthesis on the Primitive Earth. Science 130(3370):245–251, DOI 10.1126/science.130.3370.245

Mojzsis SJ, Harrison TM, Pidgeon RT (2001) Oxygen-isotope evidence from ancient zircons for liquid water at the earth's surface 4,300 myr ago. Nature 409:178 EP –, DOI 10.1038/35051557

Nesbitt R, Jahn BM, Purvis A (1982) Komatiites: An early precambrian phenomenon. Journal of Volcanology and Geothermal Research 14(1):31 – 45, DOI 10.1016/0377-0273(82)90041-5

Nisbet EG, Sleep NH (2001) The habitat and nature of early life. Nature 409(6823):1083–1091, DOI 10.1038/35059210

Pavlov AA, Kasting JF, Brown LL, Rages KA, Freedman R (2000) Greenhouse warming by CH_4 in the atmosphere of early Earth. J Geophys Res 105(E5):11981–11990, DOI 10.1029/1999JE001134

Peale SJ, Cassen P, Reynolds RT (1979) Melting of Io by Tidal Dissipation. Science 203(4383):892–894, DOI 10.1126/science.203.4383.892

Planck M (1901) Ueber das Gesetz der Energieverteilung im Normalspectrum. Annalen der Physik 309(3):553–563, DOI 10.1002/andp.19013090310

Porco CC, Helfenstein P, Thomas PC, Ingersoll AP, Wisdom J, West R, Neukum G, Denk T, Wagner R, Roatsch T, Kieffer S, Turtle E, McEwen A, Johnson TV, Rathbun J, Veverka J, Wilson D, Perry J, Spitale J, Brahic A, Burns JA, Del Genio AD, Dones L, Murray CD, Squyres S (2006) Cassini Observes the Active South Pole of Enceladus. Science 311(5766):1393–1401, DOI 10.1126/science.1123013

Ribas I, Guinan EF, Güdel M, Audard M (2005) Evolution of the Solar Activity over Time and Effects on Planetary Atmospheres. I. High-Energy Irradiances (1-1700 Å). ApJ 622(1):680–694, DOI 10.1086/427977

Rosing MT (1999) 13c-depleted carbon microparticles in $>$ 3700-ma sea-floor sedimentary rocks from west greenland. Science 283(5402):674–676, DOI 10.1126/science.283.5402.674

Sagan C (1969) Gray and Nongray Planetary Atmospheres. Structure, Convective Instability, and Greenhouse Effect. Icarus 10(2):290–300, DOI 10.1016/0019-1035(69)90030-X

Sagan C, Chyba C (1997) The early faint sun paradox: Organic shielding of ultraviolet-labile greenhouse gases. Science 276:1217–1221, DOI 10.1126/science.276.5316.1217

Sagan C, Mullen G (1972) Earth and mars: Evolution of atmospheres and surface temperatures. Science 177(4043):52–56, DOI 10.1126/science.177.4043.52

Schidlowski M (1988) A 3,800-million-year isotopic record of life from carbon in sedimentary rocks. Nature 333(6171):313–318

Selsis F, Kasting JF, Levrard B, Paillet J, Ribas I, Delfosse X (2007) Habitable planets around the star Gliese 581? A&A 476(3):1373–1387, DOI 10.1051/0004-6361:20078091

Shapiro AV, Shapiro AI, Gizon L, Krivova NA, Solanki SK (2020) Solar-cycle irradiance variations over the last four billion years. A&A 636:A83, DOI 10.1051/0004-6361/201937128

Shimizu I (2015) Past and present experiments of geoneutrinos. Physics Procedia 61:355 – 358, DOI 10.1016/j.phpro.2014.12.075, 13th International Conference on Topics in Astroparticle and Underground Physics, TAUP 2013

Smith BA, Soderblom LA, Johnson TV, Ingersoll AP, Collins SA, Shoemaker EM, Hunt GE, Masursky H, Carr MH, Davies ME, Cook I Allan F, Boyce J, Danielson GE, Owen T, Sagan C, Beebe RF, Veverka J, Strom RG, McCauley JF, Morrison D, Briggs GA, Suomi VE (1979) The Jupiter System Through the Eyes of Voyager 1. Science 204(4396):951–957, DOI 10.1126/science.204.4396.951

Solanki SK, Krivova NA, Haigh JD (2013) Solar Irradiance Variability and Climate. ARA&A 51(1):311–351, DOI 10.1146/annurev-astro-082812-141007

Spencer JR, Jessup KL, McGrath MA, Ballester GE, Yelle R (2000) Discovery of Gaseous S_2 in Io's Pele Plume. Science 288(5469):1208–1210, DOI 10.1126/science.288.5469.1208

Spohn T (1991) Mantle differentiation and thermal evolution of Mars, Mercury, and Venus. Icarus 90:222–236, DOI 10.1016/0019-1035(91)90103-Z

Stefan J (1879) Über die Beziehung zwischen der Wärmestrahlung und der Temperatur, Sitzungsberichte der Kaiserlichen Akademie der Wissenschaften in Wien, vol 79. Aus der k.k. Hof- und Staatsdruckerei

Terez EI, Terez GA (2003) A method to determine atmospheric optical depth using observations of direct solar radiation. Journal of Geophysical Research: Atmospheres 108(D22), DOI 10.1029/2003JD003829

Turcotte DL, Pflugrath JC (1985) Thermal structure of the accreting earth. Journal of Geophysical Research: Solid Earth 90(S02):C541–C544, DOI 10.1029/JB090iS02p0C541

Urey HC (1955) The cosmic abundances of potassium, uranium, and thorium and the heat balances of the earth, the moon, and mars. Proceedings of the National Academy of Sciences 41(3):127–144, DOI 10.1073/pnas.41.3.127

Valley JW, Cavosie AJ, Ushikubo T, Reinhard DA, Lawrence DF, Larson DJ, Clifton PH, Kelly TF, Wilde SA, Moser DE, Spicuzza MJ (2014) Hadean age for a post-magma-ocean zircon confirmed by atom-probe tomography. Nature Geoscience 7(3):219–223, DOI 10.1038/ngeo2075

Walker JCG (1983) Possible limits on the composition of the Archaean ocean. Nature 302(5908):518–520, DOI 10.1038/302518a0

Walker JCG, Zahnle KJ (1986) Lunar nodal tide and distance to the Moon during the Precambrian. Nature 320(6063):600–602, DOI 10.1038/320600a0

Walter MR, Buick R, Dunlop JSR (1980) Stromatolites 3,400–3,500 myr old from the north pole area, western australia. Nature 284(5755):443–445, DOI 10.1038/284443a0

Webb DJ (1980) Tides and tidal friction in a hemispherical ocean centred at the equator. Geophysical Journal 61:573–600, DOI 10.1111/j.1365-246X.1980.tb04833.x

Webb DJ (1982) Tides and the evolution of the earth-moon system. Geophysical Journal 70:261–271, DOI 10.1111/j.1365-246X.1982.tb06404.x

Wei PS, Chiu HH, Hsieh YC, Yen DL, Lee C, Tsai YC, Ting TC (2019) Absorption coefficient of water vapor across atmospheric troposphere layer. Heliyon 5(1):e01145, DOI 10.1016/j.heliyon.2019.e01145

Whitmire DP, Doyle LR, Reynolds RT, Matese JJ (1995) A slightly more massive young Sun as an explanation for warm temperatures on early Mars. J Geophys Res 100(E3):5457–5464, DOI 10.1029/94JE03080

Wilde SA, Valley JW, Peck WH, Graham CM (2001) Evidence from detrital zircons for the existence of continental crust and oceans on the earth 4.4 gyr ago. Nature 409:175 EP –, DOI 10.1038/35051550

Young GM, Brunn VV, Gold DJC, Minter WEL (1998) Earth's oldest reported glaciation: Physical and chemical evidence from the archean mozaan group (2.9 ga) of south africa. The Journal of Geology 106(5):523–538

Zahnle K, Arndt N, Cockell C, Halliday A, Nisbet E, Selsis F, Sleep NH (2007) Emergence of a Habitable Planet. Space Sci. Rev.129:35–78, DOI 10.1007/s11214-007-9225-z

Zschau J (1978) Tidal Friction in the Solid Earth: Loading Tides Versus Body Tides. In: Brosche P, Suendermann J (eds) Tidal Friction and the Earth's Rotation, p 62